Dark matter effects on tidal deformabilities and moment of inertia in a hadronic model with short-range correlations

O. Lourenço, C. H. Lenzi, T. Frederico, and M. Dutra

Departamento de Física, Instituto Tecnológico de Aeronáutica,
DCTA 12228-900, São José dos Campos, SP, Brazil

In this work, we study the outcomes related to dimensionless tidal deformability (Λ) obtained through a relativistic mean-field (RMF) hadronic model including short-range correlations (SRCs) and dark matter (DM) content [Phys. Rev. D **105**, 023008 (2022)]. As a dark particle candidate, we use the lightest neutralino interacting with nucleons through the Higgs boson exchange. In particular, we test the model against the constraints regarding the observation of gravitational waves from the binary neutron star merger event GW170817 provided by the LIGO/Virgo Collaboration (LVC). We show that Λ decreases as the dark particle Fermi momentum ($k_F^{\rm DM}$) increases. This feature favors the RMF-SRC-DM model used here to satisfy the limits of $\Lambda_{1.4} = 190_{-120}^{+390}$ (Λ of a 1.4 $M_\odot$ neutron star), and $\tilde{\Lambda} = 300_{-230}^{+420}$ given by the LVC. We also show that as $k_F^{\rm DM}$ increases, Λ_1 and Λ_2, namely, the tidal deformabilities of the binary system, are also moved in the direction of the GW170817 observational data. Finally, we verify that the inclusion of DM in the system does not destroy the *I*-Love relation (correlation between Λ and the dimensionless moment of inertia, $\bar{I}$). The observational data for $\bar{I}_\star \equiv \bar{I}(M_\star) = 11.10_{-2.28}^{+3.68}$, with $M_\star = 1.338\ M_\odot$, is obtained by the RMF-SRC-DM model.

I. INTRODUCTION

The study of strongly interacting matter in the high-density regime, i.e., for densities around somes times the nuclear saturation density (ρ_0), can be performed through the analysis of astrophysical compact objects such as neutron stars (NSs). In the last years, a huge amount of data related to these systems was provided by the LIGO/Virgo Collaboration (LVC) since their first detection of gravitational waves (GWs), a phenomenon predicted by Albert Einstein in 1916 after the formulation of general relativity [1,2]. LVC published in Ref. [3] their results regarding the GWs produced by two colliding black holes, detected in 2015 in an event called GW150914. In 2017 the event GW170817, also detected by LVC [4], was confirmed to have produced GWs from the merger of two NSs in a binary system. This former event gave rise to constraints on the tidal deformabilities of each companion star, namely, an effect analogous to the tides observed on our planet due to the presence of the Moon.

Neutron stars can also be seen as an environment with some dark matter (DM) content [5–8]. Despite the fact that the interaction between dark particles and luminous matter is extremely weak (otherwise DM would be easily detected), the gravitational force can bind this exotic matter to the ordinary matter present in massive astrophysical systems. In that direction, many investigations were performed in which DM is coupled to hadronic relativistic

mean-field (RMF) models; see Refs. [9–20] for instance. In most of these studies, the lightest neutralino, belonging to a class of weakly interacting massive particles [21,22], is used as a dark particle candidate, but there are other ones, namely, gravitinos, axinos, axions, sterile neutrinos, WIMPzillas, supersymmetric *Q*-balls, and mirror matter [21,22].

In Ref. [23] the lightest neutralino was implemented as the dark particle in a RMF model with short-range correlations (SRCs) [24–29] included. These kind of correlations are observed in electron-induced quasielastic proton knockout experiments, in which nonindependent nucleons correlate each other in pairs with high relative momentum. Probes of this phenomenon were performed in experiments at the Thomas Jefferson National Accelerator Facility, where it was found that most of the emerged pairs are deuteron-like [30], around 90% in measurements of the ^{12}C nucleus [31], for instance. Based on this RMF-SRC hadronic model, it was shown in Ref. [23] that it is possible to describe NSs with DM content presenting masses in the limits given in Ref. [32], namely, $M = 2.14_{-0.09}^{+0.10}\ M_\odot$ (68.3% credible level), and simultaneously in agreement with the recent observational data provided by NASA's Neutron star Interior Composition Explorer (NICER) mission that, provided constraints on the mass-radius profiles [33–36]. The "best" parametrizations of this RMF-SRC-DM model were constructed by taking into account the variation in the symmetry energy slope in a range compatible with the results reported

by the updated lead radius experiment (PREX-2) [37,38], and also overlapping with the boundaries obtained from the analysis of charged pions spectra [39]. The results provided in Ref. [23] are also compatible with more recent data given in Ref. [40] regarding the most massive neutron star known, namely, $M = 2.08^{+0.07}_{-0.07} M_\odot$ (68.3% credibility).

In this work, we investigate whether it is also possible to describe the constraints related to the dimensionless tidal deformabilities regarding the event GW170817 by using the RMF-SRC-DM model of Ref. [23]. In particular, we verify that the system with DM content is able to reproduce the limits of $\Lambda_{1.4} = 190^{+390}_{-120}$ [41] (dimensionless tidal deformability of a 1.4 $M_\odot$ NS), the range of $\tilde{\Lambda} = 300^{+420}_{-230}$ [42] (quantity related to the dimensionless deformabilities of the binary system stars: Λ_1 and Λ_2), and the $\Lambda_1 \times \Lambda_2$ regions. Furthermore, we also show that the I-Love relation is preserved even in the system with DM. Moreover, we find that the model also satisfies the indirect observational data related to the dimensionless moment of inertia, namely, $\bar{I}(M_\star) = 11.10^{+3.68}_{-2.28}$, with $M_\star = 1.338 M_\odot$. Regarding this last quantity, we remark that the obtained range is not coming from a directly measured observable. It is a derived quantity under certain assumptions, as we make clear later on. We organize all these findings as follows. In Sec. II, we address the main equations regarding the RMF-SRC-DM model. The predictions of the model concerning the GW170817 constraints on the tidal deformabilities and moment of inertia are given in Sec. III. Our summary and concluding remarks are presented in Sec. IV.

II. HADRONIC MODEL WITH SRC AND DM

We start by presenting the model that describes the hadronic matter considered here, defined by its Lagrangian density. It reads

$$
\begin{aligned}
\mathcal{L}_{\text{HAD}} &= \bar{\psi}(i\gamma^\mu \partial_\mu - M_{\text{nuc}})\psi + g_\sigma \sigma \bar{\psi}\psi - g_\omega \bar{\psi}\gamma^\mu \omega_\mu \psi \\
&- \frac{g_\rho}{2} \bar{\psi}\gamma^\mu \vec{\rho}_\mu \vec{\tau}\psi + \frac{1}{2}(\partial^\mu \sigma \partial_\mu \sigma - m_\sigma^2 \sigma^2) - \frac{A}{3}\sigma^3 - \frac{B}{4}\sigma^4 \\
&- \frac{1}{4}F^{\mu\nu}F_{\mu\nu} + \frac{1}{2}m_\omega^2 \omega_\mu \omega^\mu + \frac{c}{4}(g_\omega^2 \omega_\mu \omega^\mu)^2 - \frac{1}{4}\vec{B}^{\mu\nu}\vec{B}_{\mu\nu} \\
&+ \frac{1}{2}\alpha_3' g_\omega^2 g_\rho^2 \omega_\mu \omega^\mu \vec{\rho}_\mu \vec{\rho}^\mu + \frac{1}{2}m_\rho^2 \vec{\rho}_\mu \vec{\rho}^\mu.
\end{aligned}
\tag{1}
$$

In this expression ψ represents the nucleon field, and σ, ω^μ, and $\vec{\rho}_\mu$ are the scalar, vector, and isovector-vector fields related to the mesons σ, ω, and ρ, respectively, with tensors $F_{\mu\nu}$ and $\vec{B}_{\mu\nu}$ given by $F_{\mu\nu} = \partial_\nu \omega_\mu - \partial_\mu \omega_\nu$ and $\vec{B}_{\mu\nu} = \partial_\nu \vec{\rho}_\mu - \partial_\mu \vec{\rho}_\nu$. The mesons masses are m_σ, m_ω, and m_ρ. M_{nuc} is the nucleon rest mass. Regarding the inclusion of the dark matter content, we proceed as in Ref. [23] and consider a dark fermion (mass M_χ, Dirac field χ) interacting with nucleons through the exchange of the

Higgs boson (mass m_h, scalar field h). In this perspective, the Lagrangian density of the total system becomes

$$
\begin{aligned}
\mathcal{L} &= \bar{\chi}(i\gamma^\mu \partial_\mu - M_\chi)\chi + \xi h \bar{\chi}\chi + \frac{1}{2}(\partial^\mu h \partial_\mu h - m_h^2 h^2) \\
&+ f\frac{M_{\text{nuc}}}{v}h\bar{\psi}\psi + \mathcal{L}_{\text{HAD}},
\end{aligned}
\tag{2}
$$

with fM_{nuc}/v being the Higgs-nucleon coupling ($v = 246$ GeV is the Higgs vacuum expectation value). The constant ξ is the strength of the Higgs–dark particle coupling.

By using the mean-field approximation to the fields, one has $\sigma \to \langle \sigma \rangle \equiv \sigma, \omega_\mu \to \langle \omega_\mu \rangle \equiv \omega_0, \vec{\rho}_\mu \to \langle \vec{\rho}_\mu \rangle \equiv \bar{\rho}_{0(3)}$, $h \to \langle h \rangle \equiv h$, which leads to the following field equations:

$$
m_\sigma^2 \sigma = g_\sigma \rho_s - A\sigma^2 - B\sigma^3, \tag{3}
$$

$$
m_\omega^2 \omega_0 = g_\omega \rho - Cg_\omega(g_\omega \omega_0)^3 - \alpha_3' g_\omega^2 g_\rho^2 \bar{\rho}_{0(3)}^2 \omega_0, \tag{4}
$$

$$
m_\rho^2 \bar{\rho}_{0(3)} = \frac{g_\rho}{2}\rho_3 - \alpha_3' g_\omega^2 g_\rho^2 \bar{\rho}_{0(3)} \omega_0^2, \tag{5}
$$

$$
[\gamma^\mu(i\partial_\mu - g_\omega \omega_0 - g_\rho \bar{\rho}_{0(3)}\tau_3/2) - M^*]\psi = 0, \tag{6}
$$

$$
m_h^2 h = \xi \rho_s^{\text{DM}} + f\frac{M_{\text{nuc}}}{v}\rho_s, \tag{7}
$$

$$
(\gamma^\mu i\partial_\mu - M_\chi^*)\chi = 0, \tag{8}
$$

with $\tau_3 = 1$ for protons and $\tau_3 = -1$ for neutrons. The effective nucleon and dark effective masses are $M^* = M_{\text{nuc}} - g_\sigma \sigma - f\frac{M_{\text{nuc}}}{v}h$ and $M_\chi^* = M_\chi - \xi h$, respectively. Here, we use $\xi = 0.01$ and $M_\chi = 200$ GeV (lightest neutralino). Concerning f, we use the central value obtained in Ref. [43], namely, $f = 0.3$. Such a combination of values gives a spin-independent scattering cross section around 10^{-47} cm^2 [12] compatible with experimental data from the PandaX-II [44], LUX [45], and DarkSide [46] collaborations. Furthermore, the densities are given by $\rho_s = \langle \bar{\psi}\psi \rangle = \rho_{sp} + \rho_{sn}$, $\rho = \langle \bar{\psi}\gamma^0 \psi \rangle = \rho_p + \rho_n$, $\rho_3 = \langle \bar{\psi}\gamma^0 \tau_3 \psi \rangle = \rho_p - \rho_n = (2y_p - 1)\rho$, and $\rho_s^{\text{DM}} = \langle \bar{\chi}\chi \rangle$, where

$$
\rho_s^{\text{DM}} = \frac{\gamma M_\chi^*}{2\pi^2}\int_0^{k_F^{\text{DM}}} \frac{k^2 dk}{(k^2 + M_\chi^{*2})^{1/2}}. \tag{9}
$$

Here p, n defines protons and neutrons, and $\gamma = 2$ is the degeneracy factor. The proton fraction is given by $y_p = \rho_p/\rho$, with proton/neutron densities given by $\rho_{p,n} = \gamma k_{Fp,n}^3/(6\pi^2)$. $k_{Fp,n}$ and k_F^{DM} are the Fermi momenta related to protons/neutrons, and to the dark particle, respectively.

The thermodynamics of the entire system composed of hadrons and dark matter is determined from the energy density and the pressure, both of which are obtained

through the energy-momentum tensor $T^{\mu\nu}$ as $\mathcal{E} = \langle T_{00} \rangle$ and $P = \langle T_{ii} \rangle / 3$. In our case such quantities are given by

$$\mathcal{E} = \frac{m_\sigma^2 \sigma^2}{2} + \frac{A\sigma^3}{3} + \frac{B\sigma^4}{4} - \frac{m_\omega^2 \omega_0^2}{2} - \frac{C g_\omega^4 \omega_0^4}{4} - \frac{m_\rho^2 \bar{\rho}_{0(3)}^2}{2}$$
$$+ g_\omega \omega_0 \rho + \frac{g_\rho}{2} \bar{\rho}_{0(3)} \rho_3 - \frac{1}{2} \alpha_3' g_\omega^2 g_\rho^2 \omega_0^2 \bar{\rho}_{0(3)}^2 + \mathcal{E}_{\rm kin}^p + \mathcal{E}_{\rm kin}^n$$
$$+ \frac{m_h^2 h^2}{2} + \mathcal{E}_{\rm kin}^{\rm DM}, \tag{10}$$

and

$$P = -\frac{m_\sigma^2 \sigma^2}{2} - \frac{A\sigma^3}{3} - \frac{B\sigma^4}{4} + \frac{m_\omega^2 \omega_0^2}{2} + \frac{C g_\omega^4 \omega_0^4}{4}$$
$$+ \frac{m_\rho^2 \bar{\rho}_{0(3)}^2}{2} + \frac{1}{2} \alpha_3' g_\omega^2 g_\rho^2 \omega_0^2 \bar{\rho}_{0(3)}^2 + P_{\rm kin}^p + P_{\rm kin}^n - \frac{m_h^2 h^2}{2}$$
$$+ P_{\rm kin}^{\rm DM}, \tag{11}$$

with the kinetic terms of the dark particle written as

$$\mathcal{E}_{\rm kin}^{\rm DM} = \frac{\gamma}{2\pi^2} \int_0^{k_F^{\rm DM}} k^2 (k^2 + M_\chi^{*2})^{1/2} dk, \tag{12}$$

$$P_{\rm kin}^{\rm DM} = \frac{\gamma}{6\pi^2} \int_0^{k_F^{\rm DM}} \frac{k^4 dk}{(k^2 + M_\chi^{*2})^{1/2}}. \tag{13}$$

On the hadronic side of the system, the implementation of the SRC implies the replacement of the usual step functions in the kinetic terms by the one including the high-momentum tail [28,47], namely, $n_{n,p}(k) = \Delta_{n,p}$ for $0 < k < k_{Fn,p}$ and $n_{n,p}(k) = C_{n,p}(k_{Fn,p}/k)^4$ for $k_{Fn,p} < k < \phi_{n,p} k_{Fn,p}$ in which $\Delta_{n,p} = 1 - 3 C_{n,p}(1 - 1/\phi_{n,p})$, $C_p = C_0[1 - C_1(1 - 2y_p)]$, $C_n = C_0[1 + C_1(1 - 2y_p)]$, $\phi_p = \phi_0[1 - \phi_1(1 - 2y_p)]$ and $\phi_n = \phi_0[1 + \phi_1(1 - 2y_p)]$. Here, we use $C_0 = 0.161$, $C_1 = -0.25$, $\phi_0 = 2.38$ and $\phi_1 = -0.56$ [28,47]. Such change leads to modified expressions for the kinetic terms, namely,

$$\mathcal{E}_{\rm kin}^{n,p} = \frac{\gamma \Delta_{n,p}}{2\pi^2} \int_0^{k_{Fn,p}} k^2 dk (k^2 + M^{*2})^{1/2}$$
$$+ \frac{\gamma C_{n,p}}{2\pi^2} \int_{k_{Fn,p}}^{\phi_{n,p} k_{Fn,p}} \frac{k_{Fn,p}^4}{k^2} dk (k^2 + M^{*2})^{1/2},$$

$$P_{\rm kin}^{n,p} = \frac{\gamma \Delta_{n,p}}{6\pi^2} \int_0^{k_{Fn,p}} \frac{k^4 dk}{(k^2 + M^{*2})^{1/2}}$$
$$+ \frac{\gamma C_{n,p}}{6\pi^2} \int_{k_{Fn,p}}^{\phi_{n,p} k_{Fn,p}} \frac{k_{Fn,p}^4 dk}{(k^2 + M^{*2})^{1/2}}, \tag{14}$$

and

$$\rho_{sn,p} = \frac{\gamma M^* \Delta_{n,p}}{2\pi^2} \int_0^{k_{Fn,p}} \frac{k^2 dk}{(k^2 + M^{*2})^{1/2}}$$
$$+ \frac{\gamma M^* C_{n,p}}{2\pi^2} \int_{k_{Fn,p}}^{\phi_{n,p} k_{Fn,p}} \frac{k_{Fn,p}^4}{k^2} \frac{dk}{(k^2 + M^{*2})^{1/2}}. \tag{15}$$

This last quantity is the scalar density of protons and neutrons.

III. STELLAR MATTER: ANALYSIS OF THE GW170817 CONSTRAINTS

For the description of a NS of mass M, we need to solve the widely known Tolman-Oppenheimer-Volkov (TOV) equations [48,49] given by $dp(r)/dr = -[\epsilon(r) + p(r)][m(r) + 4\pi r^3 p(r)]/r^2 g(r)$ and $dm(r)/dr = 4\pi r^2 \epsilon(r)$, where $g(r) = 1 - 2m(r)/r$, whose solution is constrained to $p(0) = p_c$ (central pressure) and $m(0) = 0$. The condition of $p(R) = 0$ and $m(R) = M$ is satisfied in the star surface, with R defining the NS radius. For the equation of state (EoS) of the matter in the NS core, we use the hadronic model with SRC and DM content included. For the NS crust, we consider two regions, namely, the outer and the inner crust. For the former, we use the EoS proposed by Baym, Pethick and Sutherland (BPS) [50] in a density region of 6.3×10^{-12} fm$^{-3} \leq \rho_{\rm outer} \leq 2.5 \times 10^{-4}$ fm^{-3}. For the latter, we follow previous literature [51–57] and use a polytropic EoS of the form $p(\epsilon) = \mathcal{A} + \mathcal{B}\epsilon^{4/3}$ from 2.5×10^{-4} fm^{-3} to the transition density. The constants $\mathcal{A}$ and $\mathcal{B}$ are found by matching this polytropic formula to the BPS EoS at the interface between the outer and the inner crust, and to the EoS of the homogeneous core at the core-crust transition determined through the thermodynamical method [55–58].

In the case of systems composed of binary NSs, the phenomenon of tidal forces originated from the gravitational field takes place, with the consequence of inducing tidal deformabilities in each companion object. The particular deformations due to quadrupole moment produces GWs whose phase depends on the tidal deformability [59–61]. The first measurement of GWs detected from a NS binary, the event GW170817, is due to the LIGO/Virgo Collaboration [4]. Based on the study related to this new data, the LVC established constraints on the dimensionless tidal deformabilities Λ_1 and Λ_2 for each companion star of the binary system, as well as on the tidal deformability related to the star of $M = 1.4\, M_\odot$ ($\Lambda_{1.4}$). An updated version of the constraints regarding these quantities was published in Refs. [41,42]. Here, we test the capability of the hadronic model with SRC and DM included in satisfying these constraints provided by LVC. In order to do that, we calculate the dimensionless tidal deformability as $\Lambda = 2k_2/(3C^5)$, with $C = M/R$ (compactness). The second Love number is given by

$$k_2 = \frac{8C^5}{5}(1-2C)^2[2+2C(y_R-1)-y_R]$$
$$\times \{2C[6-3y_R+3C(5y_R-8)]$$
$$+4C^3[13-11y_R+C(3y_R-2)+2C^2(1+y_R)]$$
$$+3(1-2C)^2[2-y_R+2C(y_R-1)]\ln(1-2C)\}^{-1}, \quad (16)$$

with $y_R \equiv y(R)$. $y(r)$ is obtained through the solution of $r(dy/dr)+y^2+yF(r)+r^2Q(r)=0$, solved as part of a coupled system also containing the TOV equations. The quantities $F(r)$ and $Q(r)$ read

$$F(r) = \frac{1-4\pi r^2[\epsilon(r)-p(r)]}{g(r)}, \quad (17)$$

$$Q(r) = \frac{4\pi}{g(r)}\left[5\epsilon(r)+9p(r)+\frac{\epsilon(r)+p(r)}{v_s^2(r)}-\frac{6}{4\pi r^2}\right]$$
$$-4\left[\frac{m(r)+4\pi r^3 p(r)}{r^2 g(r)}\right]^2, \quad (18)$$

where the squared sound velocity is $v_s^2(r) = \partial p(r)/\partial\epsilon(r)$. Detailed derivations can be found in Refs. [59,62–65].

The input for the TOV equations coupled to the equation for $y(r)$ is the total equation of state of a system under charge neutrality and β equilibrium. In our case, we consider a system composed of protons, neutrons, electrons, muons and dark matter. The total energy density and pressure are given by $\epsilon = \mathcal{E} + \sum_l \epsilon_l$ and $p = P + \sum_l p_l$, with $\mathcal{E}$ and P given in Eqs. (10) and (11), respectively. The index l refer to the leptons (electrons and muons). The equations are solved by taking into account the following conditions: $\mu_n - \mu_p = \mu_e = \mu_\mu$ and $\rho_p - \rho_e = \rho_\mu$, where $\rho_l = [(\mu_l^2 - m_l^2)^{3/2}]/(3\pi^2)$ for $l = e, \mu$ (we use $m_e = 0$ and $m_\mu = 105.7$ MeV). The chemical potentials of protons, neutrons, electrons and muons are given, respectively, by μ_p, μ_n, μ_e, and μ_μ. Electron and muon densities are ρ_e, and ρ_μ. In the case of the hadronic model with SRC included, μ_p and μ_n are given by

$$\mu_{p,n} = 3C_{p,n}\left[\mu_{\text{kin}}^{p,n} - \frac{(\phi_{p,n}^2 k_{Fp,n}^2 + M^{*2})^{1/2}}{\phi_{p,n}}\right]$$
$$+4C_{p,n}k_{Fp,n}\ln\left[\frac{\phi_{p,n}k_{Fp,n}+(\phi_{p,n}^2 k_{Fp,n}^2+M^{*2})^{1/2}}{k_{Fp,n}+(k_{Fp,n}^2+M^{*2})^{1/2}}\right]$$
$$+\Delta_{p,n}\mu_{\text{kin}}^{p,n}+g_\omega\omega_0\pm\frac{g_\rho}{2}\bar{\rho}_{0_{(3)}}, \quad (19)$$

with $\mu_{\text{kin}}^{p,n} = (k_{Fp,n}^2 + M^{*2})^{1/2}$, where we have used the definitions $\mu_{p,n} = \partial\mathcal{E}/\partial\rho_{p,n}$.

As in Ref. [23], we use on the hadronic side of the model the updated version of the parametrization FSU2R [66], with the following bulk parameters at the saturation density of symmetric nuclear matter: $\rho_0 = 0.15$ fm^{-3},

$B_0 = -16.27$ MeV (binding energy), $M_0^* = 556.8$ MeV (effective nucleon mass at ρ_0), and $K_0 = 237.7$ MeV (incompressibility at ρ_0). We also use $C = 0.004$, $M_{\text{nuc}} = 939$ MeV, $m_\sigma = 497.479$ MeV, $m_\omega = 782.5$ MeV, and $m_\rho = 763$ MeV. In Ref. [23] the authors also considered uncertainties in M_0^*, K_0 and L_0 (symmetry energy slope at ρ_0). It was verified that changes in L_0 produce parametrizations that give mass-radius profiles in agreement with astrophysical observations, such as the boundaries of $M = 2.14^{+0.10}_{-0.09} M_\odot$ [32], simultaneously with recent data obtained by the NICER mission [33–36]. Here, we focus on the variation of this specific isovector quantity. In particular, we use [37]

$$L_0 = (106 \pm 37)\text{ MeV}, \quad (20)$$

range compatible with the updated results provided by the PREX-2 Collaboration concerning neutron skin thickness measurements of ^{208}Pb [38], and also overlapping with the limits determined from the analysis of charged pions spectra [39]. For each value of L_0 chosen in this variation, we fix in $\tilde{J} = 25.68$ MeV (FSU2R parametrization) the value of the symmetry energy at $\rho = 2\rho_0/3$. This value is consistent with the findings presented in Refs. [37,67]. By taking this procedure, we impose to the hadronic part of the model the linear correlation between L_0 and the symmetry energy at the saturation density, J. This is a particular relationship that has been verified in the literature; see for instance Refs. [68–72].

We start by showing in Fig. 1 the dimensionless tidal deformability generated by the RMF-SRC model with DM
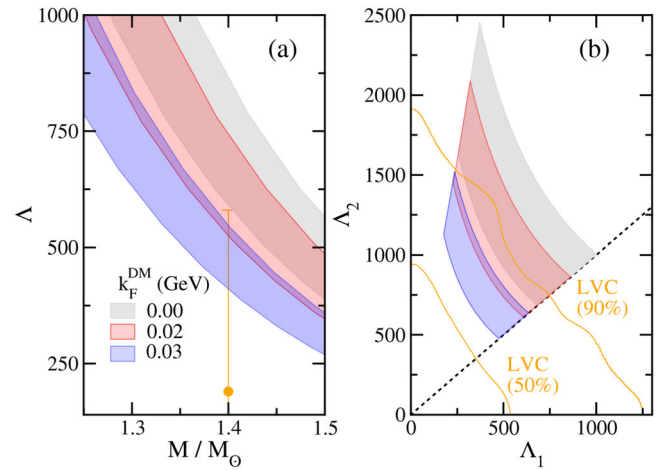

FIG. 1. (a) Λ as a function of $M/M_\odot$. Full circle: result of $\Lambda_{1.4} = 190^{+390}_{-120}$ obtained in Ref. [41]. (b) Dimensionless tidal deformabilities for the case of high-mass (Λ_1) and low-mass (Λ_2) components of the GW170817 event. Confidence lines, namely, 90% and 50%, are also taken from Ref. [41]. For both panels, the dark matter content is characterized by $k_F^{\text{DM}} = 0$ (no DM: gray bands), 0.02 GeV (red bands) and 0.03 GeV (blue bands).

included. In Fig. 1(a), we present Λ as a function of the NS mass in units of $M_\odot$. Each band represents the set of parametrizations generated by the variation of L_0 given in Eq. (20). The content of dark matter is defined by the dark Fermi momentum taken here as 0, 0.02 and 0.03 GeV. As shown in Ref. [23], $k_F^{DM} = 0$ represents the system without dark matter. It is clear that in this case (gray band), the parametrizations obtained by using Eq. (20) do not satisfy the constraint of $\Lambda_{1.4} = 190_{-120}^{+390}$ [41]. However, the inclusion of DM favors the system to be compatible with the limit provided by LVC. In particular, for $k_F^{DM} = 0.03$ GeV (blue band) it is verified that all parametrizations constructed through Eq. (20) are completely inside the range of $\Lambda_{1.4}$. This value of k_F^{DM} was shown in Ref. [23] to produce NSs in agreement with the recent observational data regarding the mass-radius diagram. Here, we confirm that the system composed of this amount of DM is also consistent with the LVC constraint of $\Lambda_{1.4}$.

In Fig. 1(b), we show the tidal deformabilities Λ_1 and Λ_2 of the binary NS system related to the event GW170817, with component masses M_1, in the range of $1.37 \leq M_1/M_\odot \leq 1.60$ [4], and $M_2 < M_1$. The diagonal dotted line corresponds to the $\Lambda_1 = \Lambda_2$ case, in which $M_1 = M_2$. The mass of the companion star is calculated through the relationship between M_1, M_2 and the chirp mass $\mathcal{M} = (M_1 M_2)^{3/5}/(M_1 + M_2)^{1/5} = 1.188\ M_\odot$ [4], i.e., $1.17 \leq M_2/M_\odot \leq 1.36$ [4,41]. The upper and lower orange lines of the figure correspond to the 90% and 50% confidence limits, respectively, also obtained from the event GW170817 [41]. From this figure, we also verify that the inclusion of DM in the system moves the bands in the direction of satisfying the LVC constraints. Notice that the system in which $k_F^{DM} = 0.03$ GeV is totally compatible with the 90% region for all values chosen for L_0 in the range of Eq. (20). These general features presented in Fig. 1 were also observed in Refs. [11,73], where other RMF-DM models were used (without SRC) including a chiral effective hadronic model. Therefore, our results point to a particular pattern regarding RMF models with DM included, at least concerning the tidal deformability. However, it is important to mention that increasing the amount of DM can also enhance Λ. This is the case of some models in which a dark matter halo [74–76] is generated. In Ref. [74], for instance, it is verified an increase of Λ for a total dark matter TOV mass (M_{DM}) exceeding $10^{-5}\ M_\odot$. In the analysis performed in Ref. [75], bosonic self-interaction dark matter was coupled to a hadronic model through a two-fluid formalism (different from that used in this work). It was shown that for DM particle masses smaller than ~300 MeV, Λ increases with the DM fraction (here, we fix the fermionic DM particle mass in 200 GeV). Finally, in Ref. [76] the authors showed that in the case of the formation of a dark matter halo, the tidal deformability increases by raising M_{DM}. The opposite situation is verified in the case of a neutron star with a DM core.

For the neutron stars described in the aforementioned works, a more sophisticated treatment of the contribution of the dark matter is performed, namely, the DM Fermi momentum is not taken as constant along the star radius. In our work, we implement the simpler case of fixing k_F^{DM} as also performed in Refs. [11,73], for instance. However, this latter treatment is completely appropriate for the purposes of the present study, namely, the investigation of tidal deformabilities and its relation with the moment of inertia.

We also performed an additional analysis by taking into account those RMF-SRC-DM parametrizations with a different range for the symmetry energy slope, namely, $40\ \text{MeV} \leq L_0 \leq 60\ \text{MeV}$, value often predicted by some hadronic models. We verified that these specific parametrizations are also compatible with the LIGO/Virgo predictions presented in Fig. 1.

In order to identify, from another perspective, the effect on $\Lambda_{1.4}$ of the DM content of the parametrizations generated from Eq. (20), we show in Fig. 2 how $\Lambda_{1.4}$ correlates with the isovector quantities L_0 and J by taking into account different values of the dark particle Fermi momentum. In Fig. 2(a), we see that $\Lambda_{1.4}$ decreases as k_F^{DM} increases, regardless of the value of L_0. The same occurs in Fig. 2(b), now with respect to the symmetry energy at the saturation density. Notice that the dependence of $\Lambda_{1.4}$ on L_0 and J reinforces the existence of a linear correlation between these two isovector quantities. Concerning $\Lambda_{1.4} \times L_0$, we remark that this pattern was also observed in a study performed in Ref. [47] in which a hadronic model with SRC but without DM was analyzed. However, notice that the inclusion of DM content reduces the increasing of $\Lambda_{1.4}$ as a function of L_0, since we have $\Delta\Lambda_{1.4} \equiv \Lambda_{1.4}(143) - \Lambda_{1.4}(69)$ given by 272, 216 and 138, respectively, for $k_F^{DM} = 0, 0.02$ and 0.03 GeV. We also remark that $\Lambda_{1.4}$ as an increasing function of J in our analysis is totally
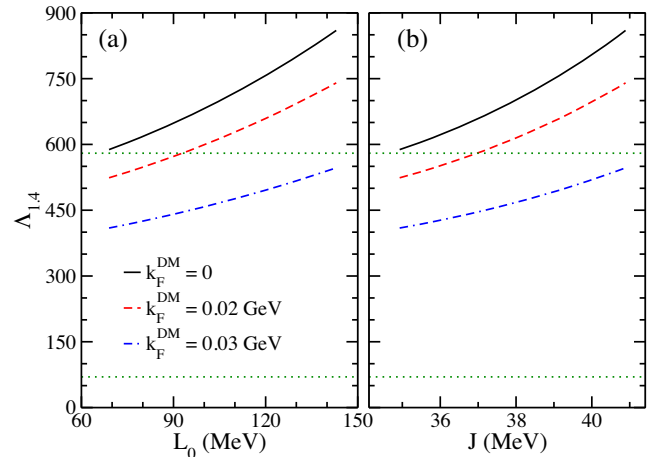

FIG. 2. $\Lambda_{1.4}$ as a function of (a) L_0 and (b) J for different values of k_F^{DM}. The range of L_0 is defined in Eq. (20). Green dotted lines: boundaries of $\Lambda_{1.4} = 190_{-120}^{+390}$ [41].

different from the correlation exhibited in Ref. [47]. In that study, the authors considered independent variations of J and L_0 and observed a decrease of $\Lambda_{1.4}$ with the increase of J. Here, the opposite behavior is verified due to the linear correlation presented between L_0 and J. This relationship emerges since, we are forcing a crossing point in the density dependence of the symmetry energy density. As aforementioned, we impose a value of 25.68 MeV for the symmetry energy at $\rho \simeq 0.1$ fm^{-3}. We refer the reader to Ref. [69] for a detailed study concerning crossing points and linear correlations of nuclear matter bulk parameters. Moreover, we emphasize that the relationship between J, L and tidal deformabilities has been the subject of investigations in many other works, such as those pointed out in Refs. [68,77–85].

A quantity directly related to the tidal deformabilities of a binary NS system is the coefficient $\tilde{\Lambda}$ defined as

$$\tilde{\Lambda} = \frac{16}{13} \frac{(M_1 + 12M_2)M_1^4\Lambda_1 + (M_2 + 12M_1)M_2^4\Lambda_2}{(M_1 + M_2)^5}, \quad (21)$$

where Λ_1 and Λ_2 are the dimensionless tidal deformabilities of each star. In the inspiral final phase of a binary colliding NS system, periodic gravitational waves are emitted. The phase of these waves can be expressed in terms of a post-Newtonian expansion yielding a term proportional to $\tilde{\Lambda}$ at the lowest order [86]. This result is used in order to investigate the response of the stellar system to the tidal field, being extracted directly from the observed waveform. In Fig. 3, we show the plots $\tilde{\Lambda} \times L_0$ and $\tilde{\Lambda} \times J$ generated through the RMF-SRC model with different DM contents. In this figure, $\tilde{\Lambda}$ is calculated as a function of the mass of one of the stars of the binary system, i.e., $\tilde{\Lambda} = \tilde{\Lambda}(M_1)$, or $\tilde{\Lambda} = \tilde{\Lambda}(M_2)$. As M_1, or M_2, is defined in a particular range according to the event GW170817,
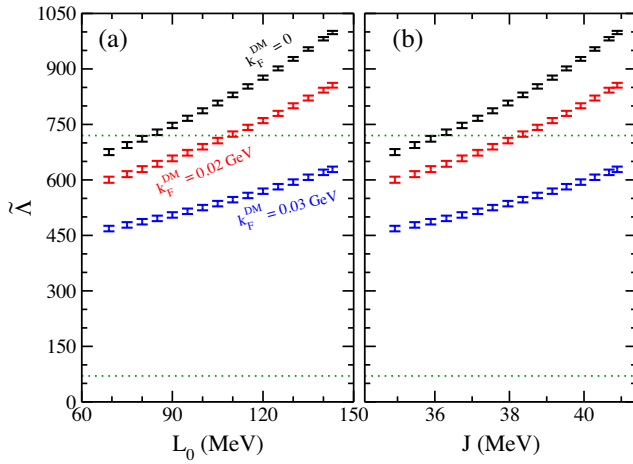
each parametrization presenting a specific value of L_0, or J, produces a range for $\tilde{\Lambda}$. We compare the results obtained for the model with $k_F^{\mathrm{DM}} = 0$, 0.02, and 0.03 GeV with the constraint $\tilde{\Lambda} = 300_{-230}^{+420}$ provided by LVC [42]. Once again, we notice that the inclusion of DM in the system favors the observational data from the event GW170817. The decreasing of $\tilde{\Lambda}$ as a function of k_F^{DM} is also observed. Furthermore, as well as the behavior between $\Lambda_{1.4}$ and L_0 depicted in Fig. 2, there is also a strong correlation between $\tilde{\Lambda}$ and L_0. The same is true for the relationship between $\tilde{\Lambda}$ and J.

As a last result, we show in Fig. 4 the dimensionless moment of inertia, $\bar{I} = I/M^3$, calculated from the RMF-SRC model for different values of k_F^{DM}. This quantity is determined from the solution of Hartle's slow rotation equation [87–89]. It is a differential equation for one of the metric decomposition functions [89], $\omega(r)$, coupled to the TOV equations. The moment of inertia is defined in terms of $\omega_R \equiv \omega(R)$ as $I = R^3(1 - \omega_R)/2$. ω_R is the frame-dragging function evaluated at the star surface [87]. The authors of Refs. [89,90] showed that the relation between $\bar{I}$ and Λ is independent of the neutron/quark star structure in the case of slowly rotating stars. In Ref. [87] the same result was obtained for a set of 53 Skyrme and RMF parametrizations. In Fig. 4(a), it is clear that the parametrizations generated by the variation in Eq. (20) are indistinguishable regardless of the value of k_F^{DM}. Therefore, we can conclude that the universal relation between $\bar{I}$ and Λ, called the I-Love relation, is preserved even with the inclusion of dark matter in the system. The dashed line in Fig. 4(a) represents the fitting curve determined in Ref. [87]. We see that the model with DM studied here is compatible with this fitting.
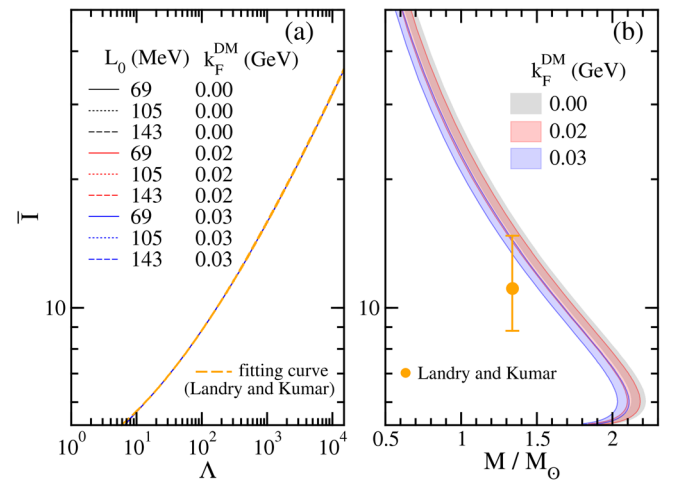

FIG. 4. Dimensionless moment of inertia as a function of (a) the dimensionless tidal deformability, and (b) the ratio $M/M_\odot$. Dashed curve: fitting curve obtained in Ref. [87]. The circle with error bars represents an indirect prediction of $\bar{I}(M = 1.338\,M_\odot)$ made in Ref. [87] by considering the observational data of the dimensionless tidal deformability (see text for more details).

FIG. 3. $\tilde{\Lambda}$ as a function of (a) L_0 and (b) J for different values of k_F^{DM}. The range of L_0 is defined in Eq. (20). Dashed lines: range of $\tilde{\Lambda} = 300_{-230}^{+420}$ determined by LVC [42].

The authors of Ref. [87] also determined a range for $\bar{I}$ related to the PSR J0737-3039 primary component pulsar, namely, $\bar{I}_\star \equiv \bar{I}(M_\star) = 11.10^{+3.68}_{-2.28}$, with $M_\star = 1.338\ M_\odot$. This range was determined by using Skyrme and RMF parametrizations. Initially, it was verified a relation between $\Lambda_\star$ (Λ related to $M_\star$) and $\Lambda_{1.4}$ (binary-Love relation). Then, a fitting for the $\Lambda_\star \times \Lambda_{1.4}$ curve was used with the I-Love relation in order to determine $\bar{I}_\star$ as a function of $\Lambda_\star$. Last, the observational range $\Lambda_{1.4} = 190^{+390}_{-120}$ from LVC was used to establish the limits for $\Lambda_\star$, and consequently, the range $\bar{I}_\star = 11.10^{+3.68}_{-2.28}$. In Fig. 4(b), we verify that the increase of k_F^{DM} produces a decrease of $\bar{I}$. We also find that the system with $k_F^{\mathrm{DM}} = 0.03$ GeV is completely inside the limits for the moment of inertia of the pulsar PSR J0737-3039A predicted in Ref. [87]. Furthermore, we verify that parametrizations generated by the RMF-SRC model, i.e., with no dark matter, are in agreement with the mass-radius diagrams obtained from chiral effective theory calculations performed in Refs. [71,91,92], for $R \lesssim 14$ km. Curiously, on the other hand, the compatibility is fully attained with the inclusion of dark matter content, specifically for $k_F^{\mathrm{DM}} = 0.03$ GeV. In summary, this specific content of dark matter, implemented in the RMF model with short-range correlations, is compatible with all constraints derived from the event GW170817 concerning the tidal deformabilities and moment of inertia.

IV. SUMMARY AND CONCLUDING REMARKS

In this work, we investigated the capability of a hadronic relativistic model, with short-range correlations and dark matter content included [23], in reproducing the observational data provided by the LIGO/Virgo Collaboration regarding the binary neutron star system of the event GW170817, i.e., the one in which gravitational waves emitted from neutron stars merger were detected. We used the lightest neutralino, interacting with nucleons through the exchange of the Higgs boson, as the dark particle. In Ref. [23] it was already shown that this model also reproduces the recent observational data obtained by the NICER mission [33–36].

We showed that the dimensionless tidal deformability Λ decreases as the Fermi momentum of the dark particle increases. In particular, this feature favors the model in satisfying the constraints of $\Lambda_{1.4} = 190^{+390}_{-120}$ and $\tilde{\Lambda} = 300^{+420}_{-230}$. Furthermore, a clear correlation between $\Lambda_{1.4}$ and the symmetry energy slope, L_0, and between $\tilde{\Lambda}$ and L_0 was verified for different values of k_F^{DM}. Specifically, we used the variation of $L_0 = (106 \pm 37)$ MeV [37], compatible with the updated results provided by the PREX-2 Collaboration concerning neutron skin thickness measurements of ^{208}Pb [38], and also overlapping with the range found from the analysis of charged pions spectra [39]. We also showed that the $\Lambda_1 \times \Lambda_2$ curves are moved in the direction of the GW170817 observational data.

Finally, we also analyzed that the I-Love relation, namely, the relationship between Λ and the dimensionless moment of inertia, $\bar{I}$, is preserved even with the inclusion of dark matter in the system. The constraint of $\bar{I}_\star \equiv \bar{I}(M_\star) = 11.10^{+3.68}_{-2.28}$, with $M_\star = 1.338\ M_\odot$, is also satisfied for the system with $k_F^{\mathrm{DM}} = 0.03$ GeV.

[1] A. Einstein, Sitzungsber. Preuss. Akad. Wiss. **1**, 688 (1916).

[2] A. Einstein, Sitzungsber. Preuss. Akad. Wiss. **1**, 154 (1918).

[3] B. P. Abbott *et al.* (LIGO Scientific Collaboration and Virgo Collaboration), Phys. Rev. Lett. **116**, 061102 (2016).

[4] B. P. Abbott *et al.* (LIGO Scientific Collaboration and Virgo Collaboration), Phys. Rev. Lett. **119**, 161101 (2017).

[5] A. Arbey and F. Mahmoudi, Prog. Part. Nucl. Phys. **119**, 103865 (2021); G. Bertonea, D. Hooperb, and J. Silk, Phys. Rep. **405**, 279 (2005).

[6] F. Zwicky, Helv. Phys. Acta **6**, 110 (1933), https://adsabs.harvard.edu/full/1933AcHPh...6..110Z/0000110.000.html.

[7] J. H. Oort, Bull. Astron. Inst. Neth. **6**, 249 (1932).

[8] L. V. Koopmans and T. Treu, Astrophys. J. **583**, 606 (2003).

[9] A. Das, T. Malik, and A. C. Nayak, Phys. Rev. D **105**, 123034 (2022).

[10] G. Panotopoulos and I. Lopes, Phys. Rev. D **96**, 083004 (2017).

[11] A. Das, T. Malik, and A. C. Nayak, Phys. Rev. D **99**, 043016 (2019).

[12] S. A. Bhat and A. Paul, Eur. Phys. J. C **80**, 544 (2020).

[13] A. Quddus, G. Panotopoulos, B. Kumar, S. Ahmad, and S. K. Patra, J. Phys. G **47**, 095202 (2020).

[14] H. C. Das, A. Kumar, B. Kumar, K. Biswal, T. Nakatsukasa, A. Li, and S. K. Patra, Mon. Not. R. Astron. Soc. **495**, 4893 (2020).

[15] H. C. Das, A. Kumar, B. Kumar, S. K. Biswal, and S. K. Patra, J. Cosmol. Astropart. Phys. 01 (2021) 007.

[16] H. C. Das, A. Kumar, and S. K. Patra, Mon. Not. R. Astron. Soc. **507**, 4053 (2021).

[17] A. G. Abac, C. C. Bernido, and J. P. H. Esguerra, arxiv: 2104.04969.

[18] H. C. Das, A. Kumar, S. K. Biswal, and S. K. Patra, Phys. Rev. D **104**, 123006 (2021).

[19] H. C. Das, A. Kumar, and S. K. Patra, Phys. Rev. D **104**, 063028 (2021).

[20] A. Kumar, H. C. Das, and S. K. Patra, Mon. Not. R. Astron. Soc. **513**, 1820 (2022).

[21] J. L. Feng, Annu. Rev. Astron. Astrophys. **48**, 495 (2010).

[22] A. Kusenko and L. J. Rosenberg, arxiv:1310.08642.

[23] O. Lourenço, T. Frederico, and M. Dutra, Phys. Rev. D **105**, 023008 (2022).

[24] M. Duer, O. Hen, E. Piasetzky *et al.*, Nature (London) **560**, 617 (2018).

[25] O. Hen, G. A. Miller, E. Piasetzky, and L. B. Weinstein, Rev. Mod. Phys. **89**, 045002 (2017).

[26] M. Duer, O. Hen, E. Piasetzky *et al.*, Phys. Lett. B **797**, 134792 (2019).

[27] B. A. Li, L. W. Chen, and C. M. Ko, Phys. Rep. **464**, 113 (2008).

[28] B. J. Cai and B. A. Li, Phys. Rev. C **93**, 014619 (2016).

[29] B. J. Cai and B. A. Li, Phys. Rev. C **105**, 064607 (2022).

[30] O. Hen *et al.*, Science **346**, 614 (2014).

[31] R. Subedi *et al.*, Science **320**, 1476 (2008).

[32] H. T. Cromartie, E. Fonseca, S. M. Ransom, P. Demorest *et al.*, Nat. Astron. **4**, 72 (2020).

[33] M. T. Wolff *et al.*, Astrophys. J. Lett. **918**, L26 (2021).

[34] M. C. Miller *et al.*, Astrophys. J. Lett. **918**, L28 (2021).

[35] T. E. Riley *et al.*, Astrophys. J. Lett. **918**, L27 (2021).

[36] G. Raaijmakers, S. K. Greif, K. Hebeler, T. Hinderer, S. Nissanke, A. Schwenk, T. E. Riley, A. L. Watts, J. M. Lattimer, and W. C. G. Ho, Astrophys. J. Lett. **918**, L29 (2021).

[37] B. T. Reed, F. J. Fattoyev, C. J. Horowitz, and J. Piekarewicz, Phys. Rev. Lett. **126**, 172503 (2021).

[38] D. Adhikari *et al.*, Phys. Rev. Lett. **126**, 172502 (2021).

[39] J. Estee *et al.*, Phys. Rev. Lett. **126**, 162701 (2021).

[40] E. Fonseca, H. T. Cromartie *et al.*, Astrophys. J. Lett. **915**, L12 (2021).

[41] B. P. Abbott *et al.* (LIGO Scientific Collaboration and Virgo Collaboration), Phys. Rev. Lett. **121**, 161101 (2018).

[42] B. P. Abbott *et al.* (LIGO Scientific Collaboration and Virgo Collaboration), Phys. Rev. X **9**, 011001 (2019).

[43] J. M. Cline, P. Scott, K. Kainulainen, and C. Weniger, Phys. Rev. D **88**, 055025 (2013); J. M. Cline, K. Kainulainen, P. Scott, and C. Weniger, Phys. Rev. D **92**, 039906(E) (2015).

[44] A. Tan *et al.* (PandaX-II Collaboration), Phys. Rev. Lett. **117**, 121303 (2016).

[45] D. S. Akerib *et al.* (LUX Collaboration), Phys. Rev. Lett. **118**, 021303 (2017).

[46] L. Marini *et al.* (DarkSide Collaboration), Nuovo Cimento C **39**, 247 (2016).

[47] L. A. Souza, M. Dutra, C. H. Lenzi, and O. Lourenço, Phys. Rev. C **101**, 065202 (2020).

[48] R. C. Tolman, Phys. Rev. **55**, 364 (1939).

[49] J. R. Oppenheimer and G. M. Volkoff, Phys. Rev. **55**, 374 (1939).

[50] G. Baym, C. Pethick, and P. Sutherland, Astrophys. J. **170**, 299 (1971).

[51] B. Link, R. I. Epstein, and J. M. Lattimer, Phys. Rev. Lett. **83**, 3362 (1999).

[52] J. Carriere, C. Horowitz, and J. Piekarewicz, Astrophys. J. **593**, 463 (2003).

[53] J. Piekarewicz and F. J. Fattoyev, Phys. Rev. C **99**, 045802 (2019).

[54] C. Gonzalez-Boquera, M. Centelles, X. Viñas, and L. M. Robledo, Phys. Lett. B **779**, 195 (2018).

[55] J. Xu, L.-W. Chen, B.-A. Li, and H.-R. Ma, Astrophys. J. **697**, 1549 (2009).

[56] J. Decharge and D. Gogny, Phys. Rev. C **21**, 1568 (1980).

[57] S. Kubis, Phys. Rev. C **70**, 065804 (2004).

[58] C. Gonzalez-Boquera, M. Centelles, X. Viñas, and T. R. Routray, Phys. Rev. C **100**, 015806 (2019).

[59] T. Hinderer, B. D. Lackey, Ryan N. Lang, and J. S. Read, Phys. Rev. D **81**, 123016 (2010).

[60] J. S. Read, L. Baiotti, J. D. E. Creighton, J. L. Friedman, B. Giacomazzo, K. Kyotoku, C. Markakis, L. Rezzolla, M. Shibata, and K. Taniguchi, Phys. Rev. D **88**, 044042 (2013).

[61] W. Del Pozzo, T. G. F. Li, M. Agathos, C. VanDenBroeck, and S. Vitale, Phys. Rev. Lett. **111**, 071101 (2013).

[62] S. Postnikov, M. Prakash, and J. M. Lattimer, Phys. Rev. D **82**, 024016 (2010).

[63] T. Hinderer, Astrophys. J. **677**, 1216 (2008).

[64] T. Damour and A. Nagar, Phys. Rev. D **81**, 084016 (2010).

[65] T. Binnington and E. Poisson, Phys. Rev. D **80**, 084018 (2009).

[66] L. Tolos, M. Centelles, and A. Ramos, Pub. Astron. Soc. Aust. **34**, e065 (2017).

[67] C. J. Horowitz and J. Piekarewicz, Phys. Rev. Lett. **86**, 5647 (2001).

[68] B. A. Li, B. J. Cai, W. J. Xie, and N. B. Zhang, Universe **7**, 182 (2021).

[69] B. M. Santos, M. Dutra, O. Lourenço, and A. Delfino, Phys. Rev. C **92**, 015210 (2015).

[70] Jin-Biao Wei, Jia-Jing Lu, G. F. Burgio, Zeng-Hua Li, and H.-J. Schulze, Eur. Phys. J. A **56**, 63 (2020).

[71] C. Drischler, A. Carbone, K. Hebeler, and A. Schwenk, Phys. Rev. C **94**, 054307 (2016).

[72] C. Drischler, R. J. Furnstahl, J. A. Melendez, and D. R. Phillips, Phys. Rev. Lett. **125**, 202702 (2020).

[73] D. Sen and A. Guha, Mon. Not. R. Astron. Soc. **504**, 3354 (2021).

[74] A. E. Nelson, S. Reddya, and D. Zhou, J. Cosmol. Astropart. Phys. 07 (2019) 012.

[75] D. R. Karkevandi, S. Shakeri, V. Sagun, and O. Ivanytskyi, Phys. Rev. D **105**, 023001 (2022).

[76] J. Ellis, G. Hütsi, K. Kannike, L. Marzola, M. Raidal, and V. Vaskonen, Phys. Rev. D **97**, 123007 (2018).

[77] B. A. Li and M. Magno, Phys. Rev. C **102**, 045807 (2020).

[78] P. G. Krastev and B. A. Li, J. Phys. G **46**, 074001 (2019).

[79] T. Malik, B. K. Agrawal, J. N. De, S. K. Samaddar, C. Providência, C. Mondal, and T. K. Jha, Phys. Rev. C **99**, 052801(R) (2019).

[80] Nai-Bo Zhang, Bin Qi, and Shou-Yu Wang, Chin. Phys. C **44**, 064103 (2020).

[81] Fan Ji, Jinniu Hu, Shishao Bao, and Hong Shen, Phys. Rev. C **100**, 045801 (2019).

[82] V. B. Thapa and M. Sinha, Phys. Rev. C **105**, 015802 (2022).

[83] J. Hu, S. Bao, Y. Zhang, K. Nakazato, K. Sumiyoshi, and H. Shen, Prog. Theor. Exp. Phys. **2020**, 043D01 (2020).

[84] H. Liu, J. Xu, and P. C. Chu, Phys. Rev. D **105**, 043015 (2022).

[85] Z. Miao, A. Li, Z. Zhu, and S. Han, Astrophys. J. **904**, 103 (2020).

[86] E. E. Flanagan and T. Hinderer, Phys. Rev. D **77**, 021502(R) (2008).

[87] P. Landry and B. Kumar, Astrophys. J. Lett. **868**, L22 (2018).

[88] J. B. Hartle, Astrophys. J. **150**, 1005 (1967).

[89] K. Yagi and N. Yunes, Phys. Rev. D **88**, 023009 (2013).

[90] K. Yagi and N. Yunes, Science **341**, 365 (2013).

[91] K. Hebeler, J. Lattimer, C. Pethick, and A. Schwenk, Astrophys. J. **773**, 11 (2013).

[92] T. Krüger, I. Tews, K. Hebeler, and A. Schwenk, Phys. Rev. C **88**, 025802 (2013).